DRAFT VERSION NOVEMBER 5, 2015
Preprint typeset using LaTeX style emulateapj v. 5/2/11

arXiv:1511.01159v1 [astro-ph.HE] 3 Nov 2015

A TALE OF TWO PULSARS AND THE ORIGIN OF TEV GAMMA RAYS FROM THE GALACTIC CENTER

MATTHEW D. KISTLER
Kavli Institute for Particle Astrophysics and Cosmology, Stanford University, SLAC National Accelerator Laboratory, Menlo Park, CA 94025
Draft version November 5, 2015

ABSTRACT

The Galactic Center (GC) has been long known to host gamma-ray emission detected to > 10 TeV. HESS data now points to two plausible origins: the supermassive black hole (perhaps with $\gtrsim$PeV cosmic rays and neutrinos) or high-energy electrons from the putative X-ray pulsar wind nebula G359.95–0.04. We show that if the magnetic field experienced by PWN electrons is near the several mG ambient field strength suggested by radio observations of the nearby GC magnetar SGR J1745-29, synchrotron losses constrain the TeV gamma-ray output to be far below the data. Accounting for the peculiar geometry of GC infrared emission, we also find that the requisite TeV flux could be reached if the PWN is ~ 1 pc from Sgr A* and the magnetic field is two orders of magnitude weaker, a scenario that we discuss in relation to recent data and theoretical developments. Otherwise, Sgr A* is left, which would then be a PeV link to other AGN.

1. INTRODUCTION

The central parsec has naturally attracted much attention, with a long history of observations utilizing the windows available to see through the Galactic disk (Genzel et al. 2010). Among the many phenomena with varying degrees of bizarreness within this region is the substantial population of compact remnants from a long history of stellar birth and death, i.e., black holes, neutron stars, and white dwarfs. However, radio surveys for pulsars have come up empty (see Dexter & O'Leary 2014; Chennamangalam & Lorimer 2014).

Evidence for a fairly powerful pulsar arose from *Chandra* observations that resolved a cometary nebula with a non-thermal X-ray spectrum, G359.95–0.04 (hereafter G359), suggestive of a pulsar wind nebula (PWN) shaped by ram pressure at a projected distance of ~ 0.3 pc from Sgr A* (Wang et al. 2006; Muno et al. 2008). The spectral steepening away from the head of the nebula is consistent with synchrotron cooling of electrons/positrons, with a 2–10 keV luminosity of $L_{\rm keV} \sim 10^{34}$ erg s^{-1} (Wang et al. 2006); however, thus far no pulsations have been reported in any band.

An intriguing possible connection is with the hard, unresolved TeV gamma-ray emission coincident with the GC seen by air Cherenkov telescopes with $L_{\rm TeV} \sim 10^{35}$ erg s^{-1} (Aharonian et al. 2004; Albert et al. 2006; Archer et al. 2014). Wang et al. (2006) suggested that multi-TeV $e^{\pm}$ producing synchrotron in the *Chandra* band are associated with the TeV gamma rays, since the ratio of ambient photon to magnetic field energy density could be large near the GC. The more detailed model of Hinton & Aharonian (2007) used a field strength of $105\,\mu$G to fit both *Chandra* and HESS data. HESS has since provided the most precise spectrum of this source (Aharonian et al. 2009) and with a much improved localization of the centroid of the emission narrowed the focus to two counterparts: Sgr A* and G359 (Acero et al. 2010).

If G359 can be demonstrated to *not* be a substantial TeV emitter, this would leave Sgr A* as the best candidate standing, from which there is no shortage of interesting scenarios for producing TeV gamma rays (see Section 5). Some of these yield high-energy neutrinos, which may well account for the PeV energy event seen by IceCube from the GC direction (Aartsen et al. 2013a). Moreover, while the Sgr A* supermassive black hole is unique in the Milky Way, it is common to massive galaxies in general and would prove an important linkage to the larger high-energy universe (Kistler 2015b).

We evaluate the viability of G359 as the source of the GC TeV gamma rays after taking into account a variety of recent data. The most stunning twist was the (unrelated) soft gamma repeater, SGR J1745-29, discovered very near Sgr A* by *Swift* (Kennea et al. 2013). *NuSTAR* detected 3.76 s X-ray pulsations (Mori et al. 2013) indicating a magnetar at ~ 2.4 arcsec (~ 0.1 pc projected) from Sgr A* (Rea et al. 2013). Of special interest is the pulsed radio emission detected with unusually large dispersion and rotation measures (Shannon & Johnston 2013). Eatough et al. (2013) concluded that the Faraday rotation results from the diffuse hot gas around the GC, with a large implied field strength of $B \gtrsim 8$ mG at the 0.1 pc scale.

It is not spoiling too much to say here that we first find that, if a mG magnetic field is germane to the synchrotron emitting $e^{\pm}$, the TeV flux obtained by normalizing to the measured X-ray flux will fall well below the HESS data. This can be simply understood from the fact that increasing B from $105\,\mu$G as in Hinton & Aharonian (2007) to $> 1000\,\mu$G increases the synchrotron loss rate by a factor of > 100, which does spoil the achievement of $L_{\rm TeV}/L_{\rm keV} \approx 10$.

Less obvious is whether conditions for TeV gamma-ray production are necessarily unsatisfactory, keeping in mind that the positional evidence for proximity to Sgr A* is more circumstantial than for objects with, e.g., orbital data. We have considered a wide variety of possibilities associated with G395 and present here several representative scenarios to illustrate a plausible range.

We focus on positions within the central parsec, since at larger distances the benefit of bright, compact infrared emission potentially producing a large $L_{\rm TeV}/L_{\rm keV}$ ratio is lost. Recent high spatial resolution measurements of the relevant infrared emission has revealed structures within the central parsec. We account for this anisotropy in TeV gamma-ray production via inverse Compton scattering and destruction due to $\gamma - \gamma$ pair production with the toy model of the GC photon field from Kistler (2015).

We examine further implications, including the consistency of the implied PWN properties with recent particle acceleration research. The *NuSTAR* discovery of very hard X-ray emission extending to > 40 keV throughout this region has a peak near G395 (Perez et al. 2015; Mori et al. 2015). We discuss the implications of synchrotron extension extending into

this range, suggestive of $\gtrsim 100$ TeV $e^{\pm}$, and the connection to gamma rays. Also, while the GC has long also been seen in GeV gamma rays, with the best observations now being from *Fermi* (Acero et al. 2015), it is not clear what is producing this emission. In the course of addressing requirements on the pulsar wind, we also will estimate the implied properties of pulsed GeV gamma rays from G359.

2. EMISSION FROM A PWN AT THE GALACTIC CENTER: I

We begin by examining simplified scenarios for producing X-rays and TeV gamma rays from G359. To do so requires some basic data. One of these is the pulsar age. The head of the G359 nebula is 8.7 arcsec from Sgr A* (~ 0.3 pc projected) and the tail approaches to with ~ 4 arcsec (Wang et al. 2006). Examining positions of known GC supernova remnants (Ponti et al. 2015) and backtracking based on the direction implied by the PWN orientation reveals no obvious correlation (SNR Sgr A East is in the opposite direction).

Wang et al. (2006) suggest an association with the IRS 13 stellar complex, which, for a $\sim$few hundred km s^{-1} relative velocity would give an age of $\sim 10^3$ yr. Lacking a characteristic spin-down age or SNR, strictly speaking we only know for certain that it was not born during the period of neutrino monitoring for Galactic SNe beginning in the 1980's (e.g., Alexeyev & Alexeyeva 2002; Ikeda et al. 2007). For instance, no supernova is recorded even from the $\lesssim 150$ yr old GC SNR G1.9+0.3 (Green et al. 2008). Hinton & Aharonian (2007) assumed a constant $e^{\pm}$ luminosity over the past 10^4 yr. For concreteness, we here use continuous injection for $\tau = 10^3$ yr.

To evolve the spectrum of these $e^{\pm}$, we use the techniques described in Kistler (2015) along with their central parsec photon field model. Once we obtain the present spectrum, we will evaluate the spectra of inverse Compton (IC) photons using each angular-dependent background component, integrating from the vantage point of the PWN over angles with respect to the direction pointing at Earth to obtain the IC spectrum as

$$\frac{dN_i}{dE_\gamma} = \mathcal{E}_i \int_{E_\gamma}^{E_{\rm max}} dE_e \frac{dN_e}{dE_0} \int d\Omega \, \frac{dN_{\rm ani}}{dE_\gamma} \ell_i(\theta,\phi)\,, \qquad (1)$$

where $\mathcal{E}_i = L_i/(4\pi c\, u_{\rm BB,i} V_i)$, with $u_{\rm BB,i}$ the blackbody energy density for a given T_i. We obtain fluxes $\varphi_i(E_\gamma)$ for each background component taking $d_{\rm GC} = 8.5$ kpc and assuming that the $e^{\pm}$ population is isotropic and relativistic beaming is not important.

We are left to determine the magnetic field relevant for the synchrotron energy loss rate and spectrum. Eatough et al. (2013) arrived at a value of $B \gtrsim 8\,(26\,{\rm cm}^{-3}/n_0)$ mG, where $n = n_0(0.4\,{\rm pc}/r)$ in the hot gas near Sgr A*, with $n_0 = 26\,{\rm cm}^{-3}$ obtained from their modeling of the GC plasma. One could simply assume that $B \sim 8$ mG throughout the entire central parsec. The implications of such a scenario can be readily extrapolated from the results of considering two possibilities for a declining field with distance from Sgr A*. The first has an equal B^2 per radial shell, $B_1(r) = 8\,(0.12\,{\rm pc}/r)$ mG. The second falls more steeply as $B_2(r) = 8\,(0.12\,{\rm pc}/r)^2$ mG.

Even the smallest of the ambient values discussed previously are much larger than typically encountered by ram pressure confined PWNe far out in the Galactic disk. Is this value typical of what is going on within G359? We will assume here that the ambient field strength is encountered by the $e^{\pm}$ after being accelerated with no field compression, discussing first evidence from the X-ray data.

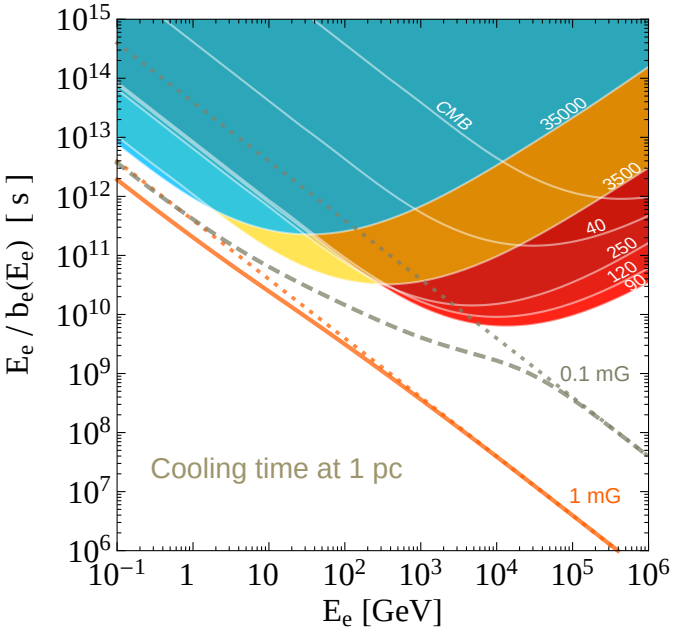

FIG. 1.— Cooling time of electrons at a distance from Sgr A* of 1 pc (*solid lines*) shown for cases with synchrotron losses for two different field strengths (*dashed lines*) and inverse Compton losses on each Galactic Center background component of the photon field from Kistler (2015).

In Fig. 1, we show both the total cooling rate and broken into components for the photon field at a distance of 1 pc from Sgr A* for two different values of B. These show how the importance of IC varies compared to synchrotron and the Klein-Nishina (KN) suppression via the break in the IC curves with increasing E_e.

As mentioned earlier, the steepening with increasing distance away from the head of the nebula measured by Wang et al. (2006) is a keystone of the PWN interpretation. They determined that to achieve a synchrotron cooling time for electrons emitting $\sim$keV X-rays comparable to the travel time along the full length of the nebula requires a field of $B \sim 0.8\,(v_f \sin i/c_s)^{2/3}$ mG, where i is the inclination of the PWN to the observer, v_f is the flow velocity, and $c_s = c/\sqrt{3}$ is the sound speed of relativistic plasma. For the nominal parameters this is consistent with a field strength in the mG range.

We can also consider the Cannonball, a PWN with similar morphology located ~ 20 pc from Sgr A* and presumed to be associated with the Sgr A East SNR. The Cannonball has been seen in hard X-rays by *NuSTAR*, from which a field of $\sim 313-530\,\mu$G was derived by Nynka et al. (2013), consistent with the ~ 0.3 mG field estimate from radio equipartition arguments in Zhao et al. (2013).

Wang et al. (2006) reported a power-law fit to the G359 X-ray spectrum with a slope of ~ -1.4 near the PWN head steepening to ~ -2, which motivates a choice of spectral index for the synchrotron emitting $e^{\pm}$ of $\alpha \gtrsim -2$. We take this as a starting point for the source spectrum, described via a smoothly-broken power law with an exponential cutoff

$$\frac{dN_e}{dE} = f_e \left[(E/E_1)^{\alpha\eta} + (E/E_1)^{\beta\eta} \right]^{1/\eta} e^{-E/E_c}\,, \qquad (2)$$

with α and β the slopes, a break at E_1, cutoff energy E_c, and $\eta = -10$ for a sharp break. In these scenarios, we assume a break at $E_1 = 1$ GeV, below which the slope is $\beta = 2$. Knowing only the projected distance, we consider three locations

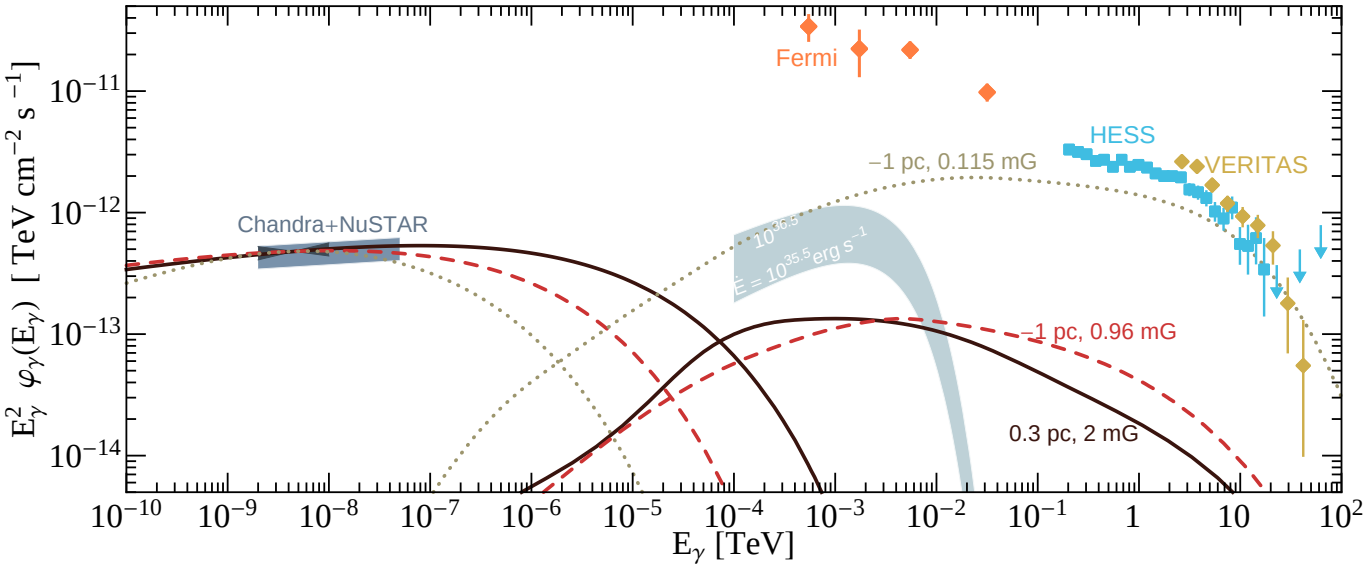

FIG. 2.— Synchrotron and inverse Compton spectra for models using a distance of 0.3 pc from Sgr A* with 2 mG field (*solid lines*) or 1 pc (behind Sgr A*) with either 0.96 mG (*dashed lines*) or 0.115 mG (*dotted lines*) and parameters in Table 1. These are compared to *Chandra* + *NuSTAR* G359 (Mori et al. 2015), *Chandra* (*bowtie*; Wang et al. 2006), the Galactic Center HESS (Viana et al. 2015) and VERITAS (Smith et al. 2015) source and *Fermi* (Acero et al. 2015) GeV source. We also estimate the pulsed $0.1-100$ GeV flux from the G359 pulsar based on the inferred PWN spindown $\dot{E} \sim 3-30\times10^{35}$ erg s^{-1} (*band*).

TABLE 1

d [pc]	B [mG]	$\mathcal{L}_{e^\pm}$ [10^{35} erg s^{-1}]	α	E_c [TeV]
0.3	2	1.19	-1.8	500
-1	0.96	1.08	-1.8	250
-1	0.115	3.05	-2.0	300

NOTE. — Parameters for our TeV gamma-ray scenarios in Fig. 2.

for G359: $d=0.3$ pc, in front of Sgr A* at $d=1$ pc, or to the rear of Sgr A* at $d=-1$ pc.

We begin at the center, $d=0.3$ pc. The above equations give $B_1(0.3\ \mathrm{pc})=3.2$ mG and $B_2(0.3\ \mathrm{pc})=1.28$ mG. We choose an intermediate value of 2 mG which well illustrates the general behavior. The $e^\pm$ luminosity, $\mathcal{L}_{e^\pm}$, and other parameters for this and subsequent scenarios are collected in Table 1. In Fig. 2 we show the results of setting the $e^\pm$ injection to match the X-ray data. Clearly, such a strong magnetic field has a much greater influence on the evolved $e^\pm$ spectrum than does the photon field at the energies of interest here. As such, the gamma-ray flux comes in well below the TeV data.

We turn to scenarios assuming locations along the same line of sight at a distance of 1 pc from Sgr A*, both in front and to the rear of Sgr A*, with much weaker magnetic fields, $B_1(1\ \mathrm{pc})=0.96$ mG and $B_2(1\ \mathrm{pc})=0.115$ mG. Taking these for both locations, the total energy loss rate is similar; however, the observed IC flux depends on the positioning of the source and scattering backgrounds relative to the observer.

In Fig. 2 we show the spectra from the 1 pc model situated behind Sgr A*. The gamma-ray flux using the larger field is again well below the TeV data. Not shown in Fig. 2 are the spectra calculated from the same distance only to the front of Sgr A*. Using the same parameters, these are similar in shape with a gamma-ray flux normalization lower by a factor of ~ 2.

The 0.115 mG case does yield a flux with the basic features, at the cost of introducing a field lower by a factor of nearly ~ 100 than that implied by the GC magnetar. Note that the X-ray flux here is not a power law, but curves through the *Chandra* flux due to our choice of exponential cutoff in combination with the other parameters. As discussed by Hinton & Aharonian (2007), with the X-ray and gamma-ray fluxes both derived from the same $e^\pm$ spectrum, which is shaped by the combined action of both loss mechanisms, it is thus relatively harder due to the KN suppression of IC. So fitting to the *Chandra* data essentially decides the shape of the gamma-ray curves and leaves little flexibility in, e.g., either forcing a sharper break above 10 TeV or accommodating a hard spectrum into the *NuSTAR* range. This can seen via the characteristic $e^\pm$ energy E_e emitting X-rays with E_X,

$$E_e \sim 20 \left(\frac{E_X}{10\,\mathrm{keV}}\right)^{1/2} \left(\frac{\mathrm{mG}}{B}\right)^{1/2} \mathrm{TeV}\,. \qquad (3)$$

While the last model displays a gamma-ray flux with desirable properties, the field strength runs into difficulties accounting for the cooling evident in *Chandra*. Also, if we had chosen the same field strength to describe the Cannonball (~ 20 pc projected) this would have been well below the derived >0.3 mG field (Nynka et al. 2013; Zhao et al. 2013). We would thus be in a situation where the synchrotron losses experienced by the PWN apparently more proximate to the GC need be roughly an order of magnitude smaller.

3. VIABILITY OF A GALACTIC CENTER PWN

This one-zone description serves to narrow down the requirements for both the synchrotron and inverse Compton fluxes to be separately compatible with the X-ray and gamma-ray data. However, lacking direct evidence via pulsed emission, a primary question remains as to whether G359 is really a PWN. If so, can the X-rays and gamma rays be consistently explained? Our aim is not to model G359 in detail, but to consider a few basic arguments in examining its viability as a PWN and a TeV gamma-ray source.

First, we recognize that the thermal and magnetic pressures are rather large in the central parsec and might rival the ram pressure for even a relatively large pulsar velocity. Assuming density $n=26(0.4\,\mathrm{pc}/r)\,\mathrm{cm}^{-3}$ and $T\sim10^7$ K (Baganoff et al. 2003; Muno et al. 2004; Wang et al. 2013), we estimate the

thermal and magnetic pressures

$$P_T = 2\,n\,k_B T \sim 10^{-7}\,\mathrm{erg\ cm^{-3}}\,,\ \mathrm{at\ 0.3\ pc}$$
$$\sim 3\times10^{-8}\,\mathrm{erg\ cm^{-3}}\,,\ \mathrm{at\ 1\ pc};$$
$$P_B = B^2/8\pi \sim 4\times10^{-8}\,(B/1\,\mathrm{mG})^2\,\mathrm{erg\ cm^{-3}}.$$

For a pulsar speed v_p, we estimate the ram pressure as

$$P_R = n\,v_p^2 \sim 1.4\times10^{-7}(v_p/500\,\mathrm{km\ s^{-1}})^2\,\mathrm{erg\ cm^{-3}},\ \mathrm{at\ 0.3\ pc}$$
$$\sim 4.3\times10^{-8}(v_p/500\,\mathrm{km\ s^{-1}})^2\mathrm{erg\ cm^{-3}}\,,\ \mathrm{at\ 1\ pc}.$$

These pressures could then all be comparable if the G359 morphology implies v_p greatly exceeding the 10^7 K sound speed, $c_s \sim 380\,\mathrm{km\ s^{-1}}$.

Lacking timing information about the pulsar, we estimate its power, $\dot{E}$, starting from the particle populations injected to account for the X-ray data (recorded in Table 1), which require $\mathcal{L}_{e^\pm} \gtrsim 10^{35}\,\mathrm{erg\ s^{-1}}$. If we assume that this results from an acceleration efficiency f_p at a shock, then

$$\dot{E} \gtrsim 10^{35}/f_p\,\mathrm{erg\ s^{-1}}\,. \tag{4}$$

The standoff distance of the termination shock of the PWN can be estimated by balancing the wind power with external pressure (e.g., Rees & Gunn 1974; Gaensler & Slane 2006) as

$$r_s = (\dot{E}/4\pi c\,P)^{1/2} \tag{5}$$
$$\sim 5\times10^{15}(\dot{E}/10^{36}\,\mathrm{erg\ s^{-1}})^{1/2}(10^{-7}\,\mathrm{erg\ cm^{-3}}/P)^{1/2}\,\mathrm{cm}$$

or $\sim 1.7\times10^{-3}$ pc. This is ~ 0.04 arcsec, consistent with no obvious extended head structure being visible in X-rays.

Since v_p is likely not much greater than c_s, we assume the distance to the back of the termination shock is comparable to r_s, $r_b \sim r_s$. The field just beyond r_s can be estimated at small wind magnetization (ratio of magnetic to particle energy fluxes), σ, following Kennel & Coroniti (1984) as $B_s \approx 3(\sigma\dot{E}/r_s^2 c)^{1/2}$ or $\sim 2.4\,\sigma^{1/2}$mG. For $\sigma = 0.01$, the 1D MHD modeling of Kennel & Coroniti (1984) displays a field strength that subsequently rises by ~ 2 up to $\sim 4\,r_s$ before slowly declining as $\sim r^{-1}$. However, the outflow confinement should arrest the decline relative to this isotropic limit.

The axisymmetric MHD simulations including ram pressure of Bucciantini et al. (2005) show a PWN structure separated into a channel with bulk velocity $v_1 \approx 0.1-0.5\,c$ surrounded by a flow with $v_2 \approx 0.8-0.9\,c$. In these models, the PWN tails are roughly cylindrical with radius $R_{\rm tail} \sim 4r_s$ and pressure $P_{\rm tail} \sim 0.02\,n\,v_p^2$. This would be smaller than P_T (and near Sgr A* even P_B) for the nominal parameters above. While this could be used to argue that G359 is well beyond the GC, since the pulsar may be the only one satisfying the criteria for observation as a PWN in the central parsec it may well possess a larger power and above average velocity. If traveling into a headwind, which for gas orbiting the GC could be substantial, it would be easier to fit into this picture.

The exact mechanism(s) of particle acceleration in PWNe remains undetermined, although recent advances offer insight into conditions that may be favorable. If the magnetic energy content of the wind is much lower than that in particles, due to dissipation prior to r_s, Fermi acceleration can redistribute energy amongst the particle population, with total number and energy being fixed. Simulations of relativistic pair shocks indicate that this is not very effective at producing hard particle spectra (Sironi et al. 2013). Alternatively, a high magnetization could permit efficient magnetic reconnection (e.g., Sironi & Spitkovsky 2014; Guo et al. 2014; Werner et al. 2014), transfer of field energy to particles, and a hard final spectrum for the population (total particle number still fixed with a increased mean energy). In either case, the where and how of particle energization from the field determine the outcome.

We proceed from $\dot{E}$, which implies a Goldreich & Julian (1969) potential $\Phi_{\rm GJ}$ and maximum energy

$$E_{\rm GJ}^{\rm max} = e\Phi_{\rm GJ} = e\,(\dot{E}/c)^{1/2}\,. \tag{6}$$

This also implies a particle flux $\dot{N}_{\rm GJ} = c\,\Phi_{\rm GJ}/e = (c\dot{E}/e)^{1/2}$ related to the total wind flux via

$$\int dE\,\frac{dN_{e^\pm}}{dE\,dt} = \dot{N} = \mathcal{M}\dot{N}_{\rm GJ}\,, \tag{7}$$

$$\int dE\,E\frac{dN_{e^\pm}}{dE\,dt} = f_p\dot{E}\,, \tag{8}$$

with pair multiplicity $\mathcal{M}$ and a bulk $\Gamma_{\rm wind} \sim \dot{E}/(m_e c^2\dot{N})$.

As determined above, $\alpha \sim -2$ is a starting point for the injected spectrum. This could plausibly be reached in acceleration via forced reconnection, which requires $\sigma \gtrsim 10$ at r_s (Sironi & Spitkovsky 2014). Traditionally, it has been a problem to dissipate the field content of the wind to get $\sigma \ll 1$ to match the detailed observations of the Crab nebula (Kennel & Coroniti 1984; cf., Porth et al. 2013). This could arise if a striped wind (with fields alternating polarity with radial distance) is able to merge and reconnect prior to r_s (e.g., Coroniti 1990; Kirk & Skjæraasen 2003). For a sufficient travel time in the wind frame to merge, $\Gamma_{\rm wind} \lesssim [(r_s/\pi r_{\rm LC})(v_w/c)]^{1/2}$ (Arons 2012), for relative velocity v_w, light cylinder radius $r_{\rm LC} = c/\Omega_p \simeq 1576\,(P_p/33\,\mathrm{ms})$ km, and pulsar period P_p.

A large pressure and $\dot{E}$ near the minimum required by the $e^\pm$ result in a small r_s, while $P_p \approx 200$ ms would place G359 in the cloud of $\dot{E} \gtrsim 10^{35}$ erg s^{-1} *Fermi* pulsars (Abdo et al. 2013), so $\Gamma_{\rm wind} \lesssim 10^3(v_w/c)^{1/2}$ for merging. This appears to be at odds with the need for TeV $e^\pm$ and $\Gamma_{\rm wind} \sim 3\times10^4$ for $\dot{E} = 10^{36}\,\mathrm{erg\ s^{-1}}$ even with $\mathcal{M} = 10^5$, so σ could remain large until $\sim r_s$. Sironi & Spitkovsky (2011) present a criterion of $4\pi\mathcal{M}\,r_{\rm LC}/r_s \gtrsim 10$ for efficient acceleration via reconnection, though they note that this requirement is generally rather difficult to accommodate in PWNe. While it is not clear how important this is to meet, this value can be approached pushing to $P_p \approx 300$ ms, $r_s \lesssim 0.5\times10^{15}$ cm, and $\mathcal{M} \gtrsim 10^5$.

4. EMISSION FROM A PWN AT THE GALACTIC CENTER: II

In light of the above, we consider a modified, yet still fairly simple, scenario for G359. In this, we assume that the accelerated $e^\pm$ enter a region with a 350 μG field in which most synchrotron losses occur, with a ~ 1 lyr length comparable to the extent of G359. Afterwards, they enter an 80 μG field, owing to either a cessation of a coherent nebula due to the high external pressure or simply reflecting a declining field strength in an extension of the nebula.

Fig. 3 shows the results of using $\alpha = -1.9$, $E_c = 100$ TeV (well below $E_{\rm GJ}^{\rm max}$ for the nominal $\dot{E}$), and injecting $\mathcal{L}_{e^\pm} = 3.5\times10^{35}$ erg s^{-1}. We again assume $\tau = 10^3$ yr, which is less relevant for X-ray synchrotron due to the short cooling time at the energies producing X-rays, although we cut the 80 μG X-ray fluxes at 30 yr to limit comparison to roughly the same spatial region.

Due to the larger synchrotron losses in the high-field region, the high-energy portion of the spectrum is burnt off prior to

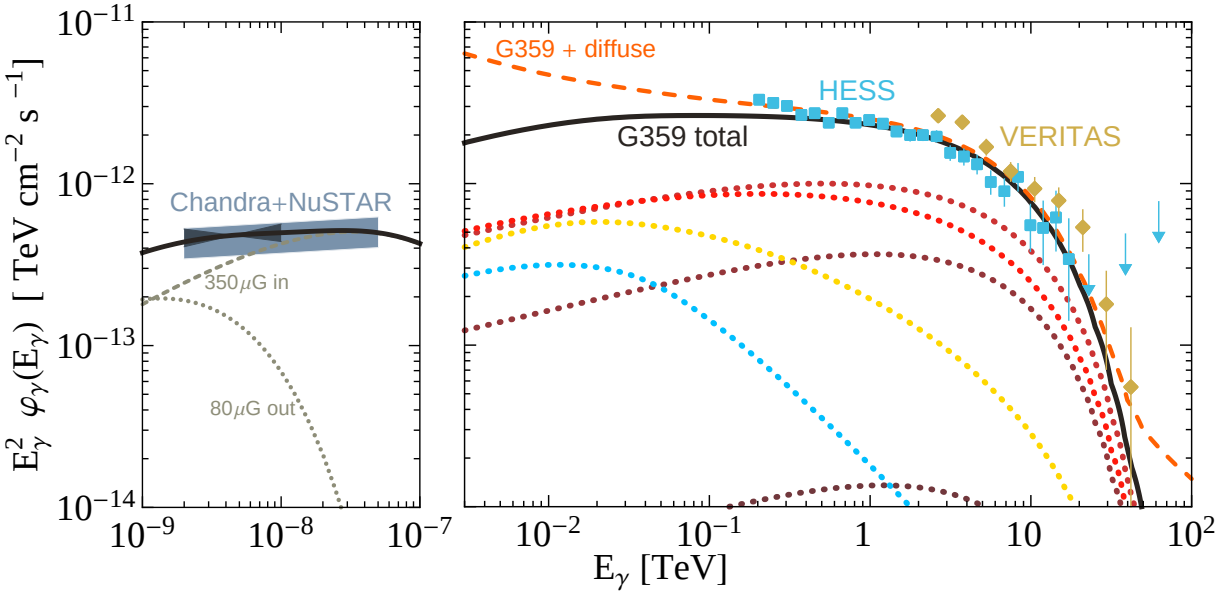

FIG. 3.— Emission spectra for the two component G359 model. *Left:* Synchrotron flux from the inner 350 μG (*dashed line*) and outer 80 μG (*dotted*) regions. *Right:* Inverse Compton from a distance of 1 pc from Sgr A* (to the rear) broken down into individual scattering background components used in Fig. 1 and their total (*solid line*) that includes $\gamma-\gamma$ attenuation, along with the addition of a diffuse component (*dashed line*; see §4).

entering the lower field where the relevance of IC increases. The resulting gamma-ray spectrum then displays a stronger than exponential cutoff, which could account for the puzzling steep drop in the 10 TeV data. The solid line in Fig. 3 includes γ–γ attenuation from Fig. 3 of Kistler (2015), while the dashed line adds a flux from hadronic interactions of an $E^{-2.5}$ proton spectrum (using the model of Kelner et al. 2006 as in Beacom & Kistler 2007) as suggested by Viana et al. (2013) if part of the diffuse TeV component identified by HESS in Aharonian et al. (2006) contributes to the source flux.

While the low energy extent of this spectrum does not affect the total energetics much, it does greatly change the implied $\mathcal{M}$. Allowing the $\alpha = -1.9$ spectrum to continue down to $E_e = 1$ GeV leads to $\mathcal{M} \sim 3\times10^4$, close to the value from above. Wang et al. (2006) and Hinton & Aharonian (2007) suggested that a lack of radio emission at G359 implies a cutoff at the low energy end of $\gtrsim$5–50 GeV. This is really all that is required to account for the X-ray and TeV emission, though leading to a much lower $\mathcal{M} \sim 100$. If radio is a problem at large downstream distances, the PWN otherwise needs to be young to avoid an accumulation of radio emitting $e^{\pm}$.

In contrast to previous assumptions, we conclude that in this scenario the TeV gamma-ray emission should *not* trace the X-ray emission of G359, since these are predominantly occurring in two distinct regions. Since the gamma rays arise much farther down the flow, they would be separated from both the PWN position and Sgr A*. The exact spatial structure in the low-field region is left to the vagaries of the local magnetic field in which the electrons are presumed to then propagate, which is discussed in relation to other data in Kistler (2015).

Although we have not explicitly constructed a dynamic model, there should be a diminution of the X-ray spectrum along with a softening, consistent with the steepening seen by Wang et al. (2006). Granted, we could also be assuming too much in interpreting from a single spectral index, as in principle the total spectrum can be the superposition of two processes, e.g., $E^{-1.5}$ and $E^{-2.5}$ over the energy range of interest, perhaps due to latitudinal dependence of the wind properties. Also, a flow separated into two channels with distinct velocities, as seen in Bucciantini et al. (2005), allows additional freedom to match details of the data.

From the $e^{\pm}$ luminosity bound on $\dot{E}$, we also estimate the pulsed gamma-ray emission of G359. This generally depends on the pulsar magnetic field geometry and the sightline to the observer. The lack of radio may imply a radio-quiet pulsar, and these have been detected by *Fermi* up to $\dot{E} \sim 5\times10^{36}$ erg s^{-1} (Abdo et al. 2013). We show in Fig. 2 the isotropic GeV flux for $\dot{E} \sim 3-30\times10^{35}$ erg s^{-1} using the estimated average spectra for this $\dot{E}$ range from O'Leary et al. (2015). This can be somewhat higher if beaming is relevant and the beam observable (e.g., Watters et al. 2009; Pierbattista et al. 2015), although the pulsed flux is likely well below the *Fermi* GC source 3FGL J1745.6–2859c (Acero et al. 2015), leaving room for other contributions, such as less powerful, but more numerous, pulsars located in this region.

5. DISCUSSION AND CONCLUSIONS

Besides novel features imposed by the properties of its surroundings at the Galactic Center, such as a potentially large external magnetic field, the putative pulsar wind nebula G359.95–0.04 is of great interest due to being situated within a TeV source also coincident with Sgr A*. A lack of strong direct evidence for Sgr A* makes it paramount to understand G359 in case the supermassive black hole actually is the accelerator yielding the gamma rays.

The several mG ambient magnetic field strength implied by data from the nearby Galactic Center magnetar, SGR J1745-29, is rather high (and possibly stronger if field reversals mask an even larger value; Eatough et al. 2013). The cooling times for high-energy electrons in such fields are quite short and there would be a meager TeV gamma-ray yield despite the GC photon field. Thus, if G359 were as close to Sgr A* as its projected 0.3 pc, one would be left with needing a much weaker field within the PWN, which would be rather peculiar in comparison to objects in the outer galaxy, where it is easy to assume that the field resulting in the synchrotron radiation

is at least as large as ambient ISM field.

If one only wished to account for the G359 *Chandra* and *NuSTAR* data, the simplest explanation may be to assume that the object is significantly beyond the Galactic Center and only apparently near Sgr A* by coincidence, thus avoiding contending with the harsh environment. Moving the PWN further out, the ambient field may be weaker; however, the field must still be strong enough to explain the observed X-ray spectral variation, and we can use this emission to gauge the $e^{\pm}$ flux and spectrum. Doing so, and assuming a uniform field and photon background similarly to (Wang et al. 2006) and Hinton & Aharonian (2007), the gamma-ray flux would still come in well below the TeV data since there would no longer be a large photon density to result in a large TeV/X-ray ratio.

Making the added assumption of a spatially varying field, we found that rough agreement can be obtained in the context of our model for a relatively narrow range of parameters, including distance, luminosity, spectra, field strengths, and assumptions about the PWN structure. For instance, in the model displayed in Fig. 3, the $e^{\pm}$ emit most of their TeV gamma rays from within a 0.08 mG field, roughly two orders of magnitude smaller than the central magnetar value. If we take the field strength of $\gtrsim 0.05$ mG derived by Crocker et al. (2010) as pervading the central ~ 100 pc as a lower bound, there would not be much additional leeway in moving the PWN much further than ~ 1 pc due to the declining background photon densities.

Considering as well the interest in the GC for reasons ranging from dark matter annihilations yielding GeV gamma rays (e.g., Abazajian et al. 2014; Daylan et al. 2014; Calore et al. 2015) and the origin of the *Fermi* bubbles (Su et al. 2010; Ackermann et al. 2014), as well as understanding multi-TeV $e^{\pm}$ production by pulsars throughout the galaxy (see, e.g., Yuksel et al. 2009; Kistler et al. 2012), it is important to understand the $e^{\pm}$ population present. It would be of great benefit to be able to perform a detailed spatial/spectral analysis as for other objects (e.g., Van Etten & Romani 2011; An et al. 2014; Gelfand et al. 2015) or to examine the X-ray data for time variability as a sign of bulk motion.

How might we proceed on G359? Radio observations have revealed the proper motion of the GC magnetar relative to Sgr A* to be ~ 6 mas yr^{-1}, a ~ 236 km s^{-1} transverse velocity (Bower et al. 2015), while pulsar speeds of $v_p \gtrsim 1000$ km s^{-1} are not unprecedented (e.g., Chatterjee et al. 2005; Ng et al. 2012; Halpern et al. 2014). For G359, $v_p \sin i \sim 700$ km s^{-1} would imply $\sim 0.2''$ per decade, measurement of which would be strong evidence of a fast pulsar, perhaps even in X-rays over a decent interval.

Also, a variety of models yield TeV gamma rays either from Sgr A* or via cosmic ray interactions in the immediate environment (e.g., Atoyan & Dermer 2004; Aharonian & Neronov 2005; Quataert & Loeb 2005; Liu et al. 2006; Ballantyne et al. 2007, 2011; Linden & Profumo 2012; Kusunose & Takahara 2012; Yusef-Zadeh et al. 2013; Fujita et al. 2015). Many of these yield neutrinos (Crocker et al. 2005; Kistler & Beacom 2006), which do not result from a leptonic PWN model, and can be searched for in IceCube (Aartsen et al. 2013a,b, 2014) or a km^3 Mediterranean detector (Coniglione 2015).

We thank Jon Arons, John Beacom, Roger Romani, Carl Farbeman, and Hasan Yuksel for useful discussions and advice. MDK acknowledges support provided by Department of Energy contract DE-AC02-76SF00515, and the KIPAC Kavli Fellowship made possible by The Kavli Foundation.

REFERENCES

Aartsen, M. G., et al. [IceCube Collaboration] 2013a, Phys. Rev. Lett., 111, 021103
Aartsen, M. G., et al. [IceCube Collaboration] 2013b, Science, 342, 1242856
Aartsen, M. G., et al. [IceCube Collaboration] 2014, Phys. Rev. Lett., 113, 101101
Abazajian, K. N., Canac, N., Horiuchi, S., & Kaplinghat, M. 2014, Phys. Rev. D, 90, 023526
Abdo, A. A., et al. [Fermi-LAT Collaboration] 2013, ApJS, 208, 17
Acero, F., et al. [HESS Collaboration] 2010, MNRAS, 402, 1877
Acero, F., et al. [Fermi-LAT Collaboration] 2015, ApJS, 218, 23
Ackermann, M., et al. [Fermi-LAT Collaboration] 2014, ApJ, 793, 64
Aharonian, F., et al. [HESS Collaboration] 2004, A&A, 425, L13
Aharonian, F., et al. [HESS Collaboration] 2006, Nature, 439, 695
Aharonian, F., et al. [HESS Collaboration] 2009, A&A, 503, 817
Aharonian, F., & Neronov, A. 2005, ApJ, 619, 306
Albert, J., et al. [MAGIC Collaboration] 2006, ApJ, 638, L101
Alexeyev, E. N., & Alexeyeva, L. N. 2002, J. Exp. Theor. Phys., 95, 5
Amato, E., & Arons, J. 2006, ApJ, 653, 325
An, H., Madsen, K. K., Reynolds, S. P., et al. 2014, ApJ, 793, 90
Archer, A., et al. [VERITAS Collaboration] 2014, ApJ, 790, 149
Arons, J. 2012, Space Sci. Rev., 173, 341
Atoyan, A., & Dermer, C. D. 2004, ApJ, 617, L123
Baganoff, F. K., Maeda, Y., Morris, M., et al. 2003, ApJ, 591, 891
Ballantyne, D. R., Melia, F., Liu, S., & Crocker, R. M. 2007, ApJ, 657, L13
Ballantyne, D. R., Schumann, M., & Ford, B. 2011, MNRAS, 410, 1521
Beacom, J. F., & Kistler, M. D. 2007, Phys. Rev. D, 75, 083001
Bower, G. C., Deller, A., Demorest, P., et al. 2015, ApJ, 798, 120
Bucciantini, N., Amato, E., & Del Zanna, L. 2005, A&A, 434, 189
Calore, F., Cholis, I., McCabe, C., & Weniger, C. 2015, Phys. Rev. D, 91, 063003
Chatterjee, S., Vlemmings, W. H. T., Brisken, W. F., et al. 2005, ApJ, 630, L61
Chennamangalam, J., & Lorimer, D. R. 2014, MNRAS, 440, L86
Chernyakova, M., Malyshev, D., Aharonian, F. A., Crocker, R. M., & Jones, D. I. 2011, ApJ, 726, 60
Coniglione, R. [KM3NeT Collaboration], 2015, J. Phys. Conf. Ser., 632, 012002
Coroniti, F. V. 1990, ApJ, 349, 538
Crocker, R. M., Melia, F., & Volkas, R. R. 2005, ApJ, 622, L37
Crocker, R. M., Jones, D. I., Melia, F., Ott, J., & Protheroe, R. J. 2010, Nature, 463, 65
Daylan, T., Finkbeiner, D. P., Hooper, D., et al. 2014, arXiv:1402.6703
Dexter, J., & O'Leary, R. M. 2014, ApJ, 783, L7
Eatough, R. P., Falcke, H., Karuppusamy, R., et al. 2013, Nature, 501, 391
Fujita, Y., Kimura, S. S., & Murase, K. 2015, Phys. Rev. D, 92, 023001
Gaensler, B. M., & Slane, P. O. 2006, ARA&A, 44, 17
Gelfand, J. D., Slane, P. O., & Temim, T. 2015, ApJ, 807, 30
Genzel, R., Eisenhauer, F., & Gillessen, S. 2010, Rev. Mod. Phys., 82, 3121
Goldreich, P., & Julian, W. H. 1969, ApJ, 157, 869
Green, D. A., Reynolds, S. P., Borkowski, K. J., Hwang, U., Harrus, I., & Petre, R. 2008, MNRAS, 387, L54
Guo, F., Li, H., Daughton, W., & Liu, Y.-H. 2014, Phys. Rev. Lett., 113, 155005
Halpern, J. P., Tomsick, J. A., Gotthelf, E. V., et al. 2014, ApJ, 795, L27
Harrison, F. A., Craig, W. W., Christensen, F. E., et al. 2013, ApJ, 770, 103
Hinton, J. A., & Aharonian, F. A. 2007, ApJ, 657, 302
Ikeda, M., et al. [Super-Kamiokande Collaboration] 2007, ApJ, 669, 519
Kelner, S. R., Aharonian, F. A., & Bugayov, V. V. 2006, Phys. Rev. D, 74, 034018
Kennea, J. A., Burrows, D. N., Kouveliotou, C., et al. 2013, ApJ, 770, L24
Kennel, C. F., & Coroniti, F. V. 1984, ApJ, 283, 694
Kirk, J. G., & Skjæraasen, O. 2003, ApJ, 591, 366
Kistler, M. D., & Beacom, J. F. 2006, Phys. Rev. D, 74, 063007
Kistler, M. D., Yuksel, H., & Friedland, A. 2012, arXiv:1210.8180
Kistler, M. D. 2015, just appeared
Kistler, M. D. 2015b, to appear
Kusunose, M., & Takahara, F. 2012, ApJ, 748, 34

Linden, T., & Profumo, S. 2012, ApJ, 760, 23
Liu, S., Melia, F., Petrosian, V., & Fatuzzo, M. 2006, ApJ, 647, 1099
Mori, K., Gotthelf, E. V., Zhang, S., et al. 2013, ApJ, 770, L23
Mori, K., Hailey, C. J., Krivonos, R., et al. 2015, arXiv:1510.04631
Muno, M. P., Baganoff, F. K., Bautz, M. W., et al. 2004, ApJ, 613, 326
Muno, M. P., Baganoff, F. K., Brandt, W. N., Morris, M. R., & Starck, J.-L. 2008, ApJ, 673, 251
Ng, C.-Y., Bucciantini, N., Gaensler, B. M., et al. 2012, ApJ, 746, 105
Nynka, M., Hailey, C. J., Mori, K., et al. 2013, ApJ, 778, L31
O'Leary, R. M., Kistler, M. D., Kerr, M., & Dexter, J. 2015, arXiv:1504.02477
Perez, K., Hailey, C. J., Bauer, F. E., et al. 2015, Nature, 520, 646
Pierbattista, M., Harding, A. K., Grenier, I. A., Johnson, T. J., Caraveo, P. A., Kerr, M., & Gonthier, P. L. 2015, A&A, 575, A3
Ponti, G., Morris, M. R., Terrier, R., et al. 2015, MNRAS, 453, 172
Porth, O., Komissarov, S. S., & Keppens, R. 2013, MNRAS, 431, L48
Quataert, E., & Loeb, A. 2005, ApJ, 635, L45
Rea, N., Esposito, P., Pons, J. A., et al. 2013, ApJ, 775, L34
Rees, M. J., & Gunn, J. E. 1974, MNRAS, 167, 1
Shannon, R. M., & Johnston, S. 2013, MNRAS, 435, L29
Sironi, L., & Spitkovsky, A. 2011, ApJ, 741, 39
Sironi, L., Spitkovsky, A., & Arons, J. 2013, ApJ, 771, 54
Sironi, L., & Spitkovsky, A. 2014, ApJ, 783, L21
Smith, A. W., et al. [VERITAS Collaboration] 2015, arXiv:1508.06311
Su, M., Slatyer, T. R., & Finkbeiner, D. P. 2010, ApJ, 724, 1044
Van Etten, A., & Romani, R. W. 2011, ApJ, 742, 62
Viana, A. & Moulin, E. [HESS Collaboration] 2013, Proc. 33rd Int. Cosmic Ray Conf., 9, 1
Viana, A. [HESS Collaboration] 2015, Proc. 34rd Int. Cosmic Ray Conf., 1, 1254
Wang, Q. D., Lu, F. J., & Gotthelf, E. V. 2006, MNRAS, 367, 937
Wang, Q. D., Nowak, M. A., Markoff, S. B., et al. 2013, Science, 341, 981
Watters, K. P., Romani, R. W., Weltevrede, P., & Johnston, S. 2009, ApJ, 695, 1289
Werner, G. R., Uzdensky, D. A., Cerutti, B., Nalewajko, K., & Begelman, M. C. 2014, arXiv:1409.8262
Yüksel, H., Kistler, M. D., & Stanev, T. 2009, Phys. Rev. Lett., 103, 051101
Yusef-Zadeh, F., Hewitt, J. W., Wardle, M., et al. 2013, ApJ, 762, 33
Zhao, J.-H., Morris, M. R., & Goss, W. M., 2013, ApJ, 777, 146